Final Draft

of the original manuscript

Li, Z.; Li, Z.; Yang, B.; He, X.; Gan, W.; Zhang, Y.; Li, Z.; Zhang, Y.; Esling, C.; Zhao, X.; Zuo, L.:

Over 2% magnetic-field-induced strain in a polycrystalline Ni50Mn28.5Ga21.5 alloy prepared by directional solidification.

In: Materials Science and Engineering: A. Vol. 780 (2020) 139170.

First published online by Elsevier: 29.02.2020

https://dx.doi.org/10.1016/j.msea.2020.139170

Over 2% magnetic-field-induced strain in a polycrystalline $Ni_{50}Mn_{28.5}Ga_{21.5}$ alloy prepared by directional solidification

Zhenzhuang Li[1], Zongbin Li[1,*], Bo Yang[2], Xijia He[3], Weimin Gan[4], Yuanlei Zhang[3], Zhe Li[3], Yudong Zhang[5], Claude Esling[5], Xiang Zhao[1], Liang Zuo[1,*]

[1]*Key Laboratory for Anisotropy and Texture of Materials (Ministry of Education), School of Materials Science and Engineering, Northeastern University, Shenyang 110819, China*

[2]*State Key Laboratory of Rolling and Automation, Northeastern University, Shenyang, 110819, China*

[3]*Center for Magnetic Materials and Devices & Key Laboratory for Advanced Functional and Low Dimensional Materials of Yunnan Higher Education Institute, Qujing Normal University, Qujing 655011, China*

[4]*German Engineering Materials Science Centre (GEMS), Helmholtz-Zentrum Geesthacht (HZG) Outstation at FRM II, D-85748, Garching, Germany*

[5]*Laboratoire d'Étude des Microstructures et de Mécanique des Matériaux (LEM3), CNRS UMR 7239, Université de Lorraine, 57045 Metz, France*

**Corresponding author.*

E-mail: *lizongbin@126.com (Zongbin Li), lzuo@mail.neu.edu.cn (Liang Zuo)*

Abstract: Ni-Mn-Ga single crystal alloys can exhibit giant magnetic shape memory effect through variant reorientation induced by the magnetic field. However, such effect is greatly weakened in polycrystalline alloys, due to the orientation differences of martensite variants and the constraints of grain boundaries. Here, to improve the magnetic shape memory effect, a polycrystalline $Ni_{50}Mn_{28.5}Ga_{21.5}$ alloy with coarse columnar shaped grains and strong $<0\ 0\ 1>_A$ texture is prepared by directional solidification. With the aids of mechanical training, the twinning stress of five-layered modulated (5M) martensite in the directionally solidified $Ni_{50}Mn_{28.5}Ga_{21.5}$ alloy is successfully lowered to ~0.9 MPa. A giant magnetic field induced strain up to ~2.1% is achieved under the magnetic field of 1 T, being much higher than those reported previously in polycrystalline alloys. In addition, a reversible magnetostrain of ~0.4% is also attained without the assistance of an external stress or a magnetic field. It is demonstrated that the microstructure control through directional solidification as well as mechanical training could be an effective solution to enhance the magnetic field induced output strain in polycrystalline Ni-Mn-Ga alloys.

Keywords: Ni-Mn-Ga alloys; Magnetic shape memory effect; Variant reorientation; Mechanical training; Microstructure control

1. Introduction

Heusler-type Ni-Mn-Ga ferromagnetic shape memory alloys have attracted much attention due to their remarkable magnetic shape memory effect in the martensitic state [1-14]. Such effect, namely the magnetic field induced strain (MFIS), is originated from the magnetically induced variant reorientation [9]. Since the first report of a MFIS of ~0.19% in Ni_2MnGa single crystal by Ullakko *et al.* [1], numerous experimental studies have been motivated to enhance the magnetic field induced output strain in these alloys [2-9]. So far, the MFIS values have almost reached the theoretical limit in single crystals, *i.e.* ~7% [6], ~11% [7] and ~12% [5] for five-layered modulated (5M), seven-layered modulated (7M) and non-modulated (NM) martensite, respectively.

Although the single crystal Ni-Mn-Ga alloys possess superior magnetic shape memory properties, the complicated and costly process for the preparation of single crystals represents a substantial hindrance for their practical applications. In contrast, the preparation of polycrystalline Ni-Mn-Ga alloys is much simple and of high productivity. However, the orientation differences of martensite variants and the pinning effect of grain boundaries impose strong constraint on the magnetic field induced variant reorientation and the resultant MFIS. For example, very low MFIS values of 0.025%, 0.016% and 0.012% were observed in $Ni_{50}Mn_{27}Mn_{23}$ melt-spun ribbon [15], $Ni_{55}Mn_{20.6}Ga_{24.4}$ melt-spun ribbon [16] and $Ni_{53}Mn_{23.5}Ga_{23.5}$ bulk alloy [17], respectively. From the technological point of view, it becomes much more demanding but truly challenging to develop high-performance polycrystalline Ni-Mn-Ga alloys.

One of the possible breakthroughs to enhance MFIS levels in polycrystalline Ni-Mn-Ga alloys is to produce coarse grained and highly textured microstructure through directional solidification [10], by which the internal constraints on the field induced variant reorientation can be significantly reduced. Previous efforts have demonstrated that the directionally solidified Ni-Mn-Ga alloys can exhibit enhanced MFIS as compared to melt-spun ribbons and bulk alloys with fine grains. Liang *et al.* reported a MFIS of 0.115% in a directionally solidified $Ni_{50.5}Mn_{24}Ga_{25.5}$ alloy [18], and Pötschke *et al.* observed a MFIS of 0.16% in a directionally solidified $Ni_{50}Mn_{29}Ga_{21}$ alloy [19]. More significant progress was achieved by Gaitzsch *et al.* [20], who reported a large MFIS up to 1% in a directionally solidified $Ni_{50}Mn_{29}Ga_{21}$ alloy.

It should be mentioned that the acquisition of MFIS is strongly dependent on the external field training [8, 20-22]. It is known that a prerequisite for obtaining large MFIS through the magnetically driven variant reorientation is that the magnetic stress provided by the external magnetic field should be higher than the twinning stress (*i.e.*, the stress to move a twin boundary) [20, 23]. In this regard, the twinning stress should be as low as possible. Nevertheless, for the martensite with self-accommodated multi-variant microstructure after martensitic transformation, the twinning stress is at a relatively high level due to the interlocking arrangement of differently oriented variants. Thus, appropriate external field training towards lowering the twinning stress becomes quite necessary [8, 20-22]. Among various training methods, the so-called mechanical training *via* cyclic deformation in orthogonal directions is considered to be the most efficient one. Especially, through repeated compressions along the $<0\ 0\ 1>_A$ axes of austenite in the single crystal alloys, the effective reduction in variant number and twinning stress can result in giant MFIS [20, 21, 24, 25]. However, for the polycrystalline alloys, the corresponding microstructure optimization and property improvement based on the mechanical training are still quite challenging, because the microstructure complexity and orientation diversity make it difficult to precisely control the loading direction, resulting in less effective in reducing the twinning stress when compared to the situation in single crystal alloys.

In this work, in order to improve the MFIS, a polycrystalline $Ni_{50}Mn_{28.5}Ga_{21.5}$ alloy was prepared by directional solidification, where the initial austenite formed the coarse columnar shaped grains and strong preferred orientation. Through the effective manipulation of mechanical training *via* cyclic compressions in two perpendicular directions, the twinning stress of 5M martensite in the directionally solidified alloy was reduced to ~0.9 MPa. Consequently, a large one-way MFIS up to ~2.1% was achieved. Such value is much higher than those in polycrystalline alloys reported previously. In addition, a reversible MFIS of ~0.4% was also obtained with no need of additional stress or magnetic field. Such distinct feature may make polycrystalline Ni-Mn-Ga alloys more competitive in practical applications.

2. Experimental

Polycrystalline Ni-Mn-Ga alloy with the nominal composition of $Ni_{50}Mn_{28.5}Ga_{21.5}$ (at. %) was prepared by directional solidification with a growth rate of 3 mm/min. Under this circumstance, the initial austenite grains had a strong $<0\ 0\ 1>_A$ preferential orientation in parallel to the solidification direction (SD). In order to achieve better homogenization of chemical composition, the as-solidified ingot was sealed in a vacuum quartz tube and held isothermally at 1173 K for 24 h, followed by quenching into water. Parts of the as-homogenized ingot were ground into powders for crystal structure analyses using powder X-ray diffraction (XRD). To remove the internal stress induced by grinding, the powders were annealed at 873 K for 5 h in a vacuum quartz tube. Several rectangular parallelepiped samples with the dimension of 4 mm × 4 mm × 5 mm were cut out of the as-homogenized ingot for mechanical training. The longer edges of samples were parallel to the SD, *i.e.*, corresponding to the <0 0 1>$_A$ preferential direction, and the short edges were also chosen to achieve the best possible alignment with <0 0 1>$_A$ axes according to the texture measurements.

The forward and inverse martensitic transformations of the examined alloy were detected by differential scanning calorimetry (DSC) in the temperature range from 183 K to 473 K, with a cooling and heating rate of 10 K/min. The start and finish transformation temperatures were determined to be 308 K (M_s), 301 K (M_f), 317 K (A_s) and 323 K (A_f), respectively. The powder XRD data were recorded using Cu-K_α radiation at the room temperature. The pole figures were measured by XRD at the room temperature on the transverse section of the directionally solidified alloy. The microstructural observations were performed in a JEOL JSM-7001F scanning electron microscope (SEM) with an EBSD camera and Channel 5 software. The *in-situ* neutron diffraction patterns during compressive loading were measured using the STRESS-SPEC Diffractometer operated by FRM II and HZG at the Heinz Maier-Leibnitz Zentrum (MLZ), Garching, Germany, with a monochromatic wavelength of 2.1 Å [26, 27]. The SteCa software was used to extract diffraction patterns from the recorded 2D diffraction images [28]. The mechanical training through alternate uniaxial compressions along two orthogonal axes (*i.e.*, parallel and perpendicular to the SD) was performed in a universal material testing machine with a loading rate of 1 N/s.

The MFIS values were measured by a self-designed experimental setup with a laser system, as schematically shown in Fig. 1. Under this frame, the strain measurement direction is perpendicular to the magnetic field. The field-induced change in length (*i.e.*, $\Delta L = \Delta L_1 + \Delta L_2$, as marked in Fig. 1) is detected with two laser displacement sensors by monitoring the variations in the reflected laser path. Accordingly, the MFIS can be calculated according to $\varepsilon = \Delta L/L \times 100\% = (\Delta L_1 + \Delta L_2)/L \times 100\%$. As the blocking stress for variant reorientation in Ni-Mn-Ga alloys is only about 2-5 MPa [29, 30], such non-contact measurement method has an advantage over the contact-type measurement (*e.g.* strain gauge) [31] in revealing the full potential of MFIS in polycrystalline alloys [32].

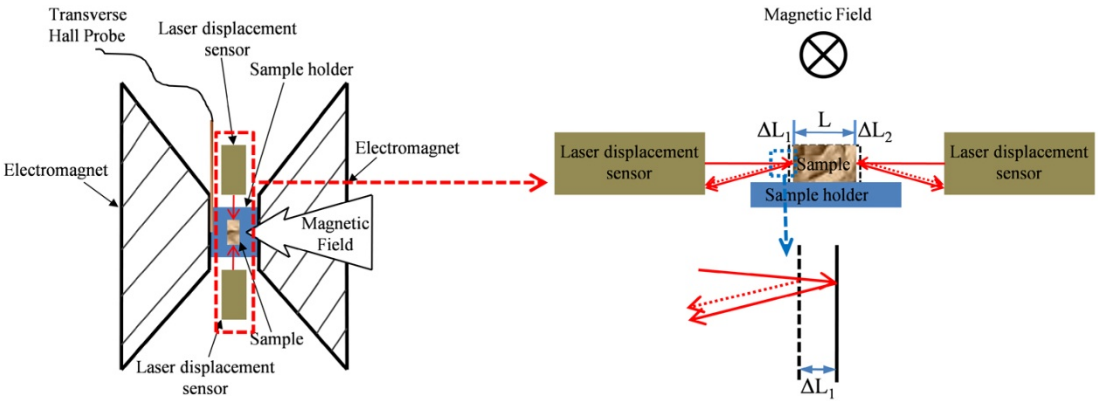

Fig. 1. Schematic of the experimental setup for MFIS measurements with two laser displacement sensors.

3. Results and discussion

3.1. Microstructural features and preferential orientation

For the present directionally solidified $Ni_{50}Mn_{28.5}Ga_{21.5}$ alloy, the room temperature phase was identified to be 5M martensite according to powder XRD measurements, where the lattice parameters were determined to be a_{5M} = 4.226 Å, b_{5M} = 5.581 Å, c_{5M} = 21.052 Å, and β = 90.3° [12]. Under the coordinate frame of 5M martensite, the easy magnetization direction is along the *b* axis, *i.e.* the $\langle 0\ 1\ 0\rangle_{5M}$ direction. It is noted that the $\langle 0\ 1\ 0\rangle_{5M}$ direction also corresponds to the favorable axis under compressive stress, *i.e.*, the so-called short axis [29].

Fig. 2(a) shows the macroscopic microstructure of the longitudinal section for the directionally solidified alloy at the room temperature. It can be recognized that the original austenite grains are in coarse columnar-shape along the SD, with an average size of ~1 mm. Such microstructural feature is frequently observed in the directionally solidified Ni-Mn-Ga alloys [26, 33]. Indeed, the initial austenite grain boundaries would impose a strong constraint on the magnetically induced reorientation of martensite variants. In this regard, a coarse-grained microstructure is quite beneficial to reduce the internal constrains and increase the MFIS.

Fig. 2(b) displays a local backscattered electron (BSE) image for the self-accommodated 5M martensite. Typically, the 5M martensite can be characterized as the broad plates with several micrometers in width, which is consistent with the previous observations [12]. Moreover, each broad plate is composed of alternately distributed fine lamellae with thickness in the nanometer range, being identified as four types of twin-related orientation variants [12]. Apparently, the existence of a large amount of differently oriented variants would greatly increase the resistance to variant reorientation and thus decrease the MFIS values. Therefore, external field training should be introduced to reduce the variant number and simplify the microstructure.

Fig. 2(c) shows the $\{0\ 0\ 10\}_{5M}$ and $\{0\ 4\ 0\}_{5M}$ incomplete pole figures for the directionally solidified alloy measured on the transverse section by XRD. It is seen that the $\{0\ 0\ 10\}_{5M}$ poles are roughly located at the polar angle of ~40° and $\{0\ 4\ 0\}_{5M}$ poles at the center of pole figure, suggesting the existence of a strong preferred orientation in the directionally solidified alloy. Since $\{0\ 0\ 10\}_{5M}$ and $\{0\ 4\ 0\}_{5M}$ of 5M martensite are originated from $\{2\ 2\ 0\}_A$ and $\{4\ 0\ 0\}_A$ of austenite [34, 35], respectively, it can be deduced that the initial austenite possesses the strong preferred orientation with $\langle 0\ 0\ 1\rangle_A$ parallel to the SD. Therefore, the present polycrystalline

$Ni_{50}Mn_{28.5}Ga_{21.5}$ alloy formed the coarse columnar shaped grains and strong <0 0 1>$_A$ preferred orientation.

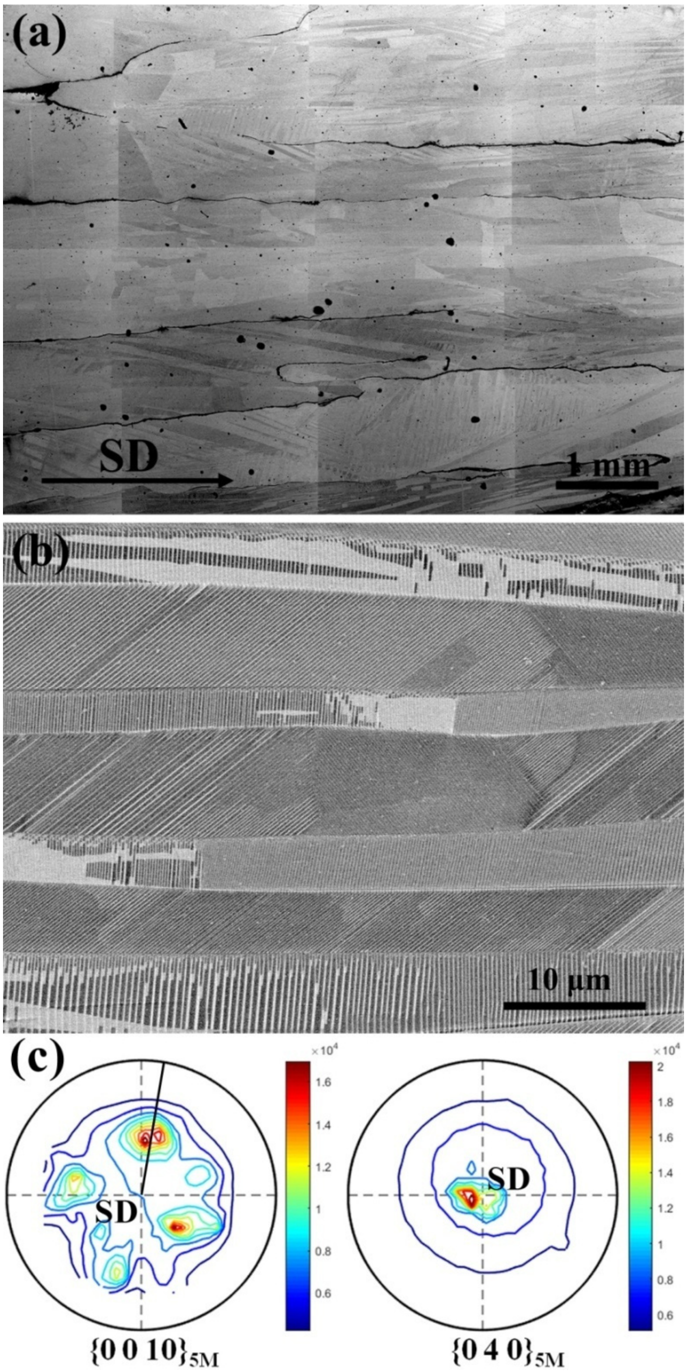

Fig. 2. (a) Macroscopic microstructure of the longitudinal section for the directionally solidified alloy (SD: solidification direction). (b) Local backscattered electron (BSE) image of 5M martensite plates. (c) {0 0 10}$_{5M}$ and {0 4 0}$_{5M}$ incomplete pole figures measured on the transverse section by XRD.

3.2. Mechanical training by cyclic compression

The twinning stress is a key parameter for achieving large MFIS through variant reorientation in Ni-Mn-Ga alloys, which should be as low as possible. Previous investigations have shown that the mechanical training through alternate uniaxial compressions along two perpendicular $<0\ 0\ 1>_A$ axes of austenite can effectively reduce the twinning stress [21]. Considering the preferred orientation of directionally solidified alloy, *i.e.*, $<0\ 0\ 1>_A$ // SD, the SD can be chosen as one compressive direction. For the effective manipulation of mechanical training, it is better that the other compressive direction in perpendicular to the SD is also along $<0\ 0\ 1>_A$ preferred orientation. Such compressive direction can be determined from the pole figures measured on the transverse section by XRD, *e.g.*, $\{0\ 0\ 10\}_{5M}$ pole figure. In the $\{0\ 0\ 10\}_{5M}$ pole figure, the line passing through the center and the poles with relatively higher intensity (as indicated in solid line in Fig. 2(c)) indicates the direction with $<0\ 0\ 1>_A$ strong preferred orientation in perpendicular to the SD, which can be selected as the other compressive direction for mechanical training.

Fig. 3 shows the compressive stress-strain curves along the two compressive directions for a representative sample. The repeated compressive loading was applied parallel to the SD for the first cycle and then perpendicular to the SD for the second cycle, and so on. It is seen that there appears stress plateau in the stress-strain curve, indicating the reorientation or detwinning of martensite variants induced by the uniaxial compression [5, 7]. Apparently, the twinning stress (determined as an external stress to achieve half of the maximum theoretical strain, *i.e.*, ~ 3% [21]) can be greatly decreased by the cyclic mechanical training. For the case of loading direction (LD) parallel to SD (Fig. 3(a)), the twinning stress was reduced from 10 MPa to 0.9 MPa. For the case of LD perpendicular to SD (Fig. 3(b)), the twinning stress was reduced from 5.5 MPa to 1.3 MPa. The much higher twinning stress associated with the first cycle of compression should be attributed to the inter-pinning of differently oriented variants, as evidenced in Fig. 2(b).

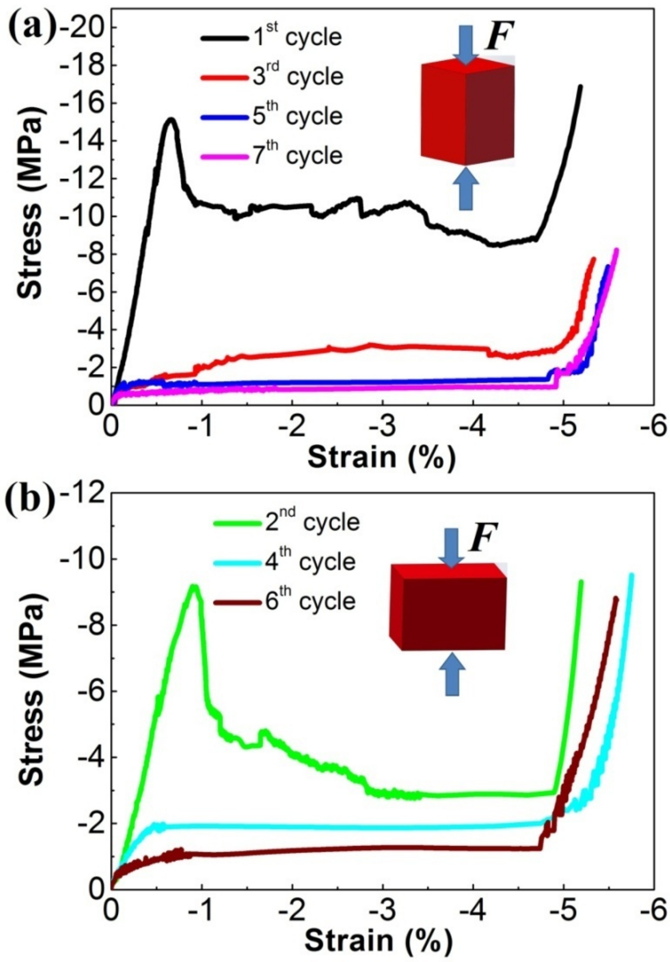

Fig. 3. Compressive stress-strain curves along two directions for the directionally solidified alloy. (a) LD//SD. (b) LD⊥SD.

In order to trace the variant reorientation behavior induced by the compressive stress, *in-situ* neutron diffraction measurements were performed. Fig. 4(a) shows the compressive stress-strain curve for an as-solidified sample, where the compressive stress was applied along the SD. The corresponding *in-situ* neutron diffraction patterns for a total of eight points marked in the stress-strain curve are shown in Fig. 4(b). Clearly, with the increase of compressive stress, the intensity of the $\{1\ 0\ 5\}_{5M}$ peaks gradually decreases, whereas the intensity of the $\{0\ 2\ 0\}_{5M}$ peaks increases.

This provides a direct evidence on variant reorientation induced by the compressive stress, where the stress-favored variants with the <0 1 0>$_{5M}$ direction parallel to the LD increase their volume fractions at the expense of the unfavorable variants.

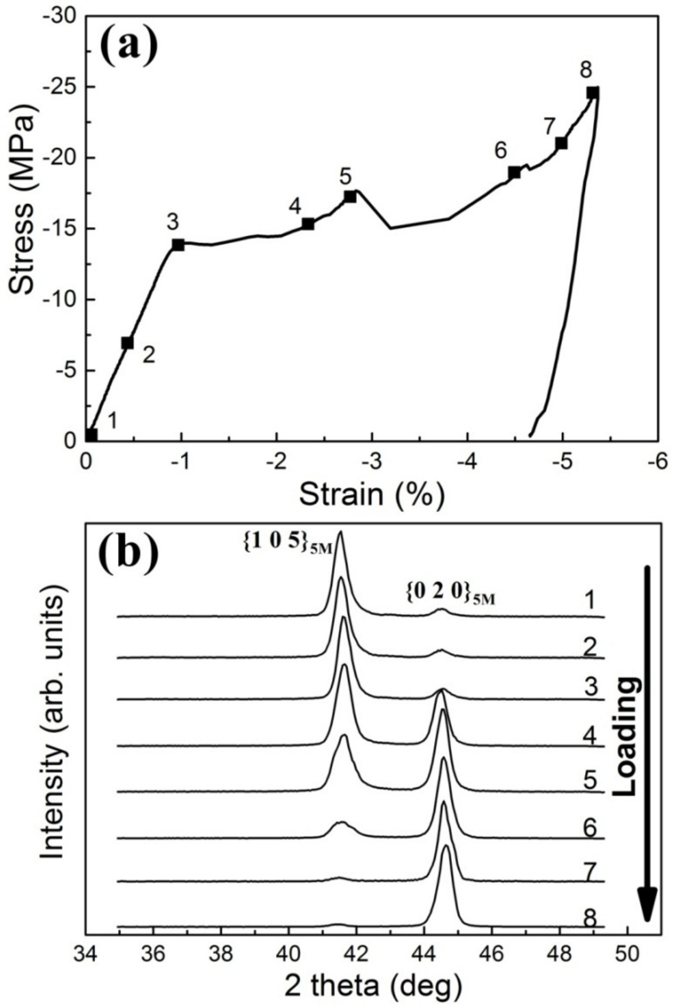

Fig. 4. *In-situ* neutron diffraction measurements during compression for the directionally solidified alloy with LD//SD. (a) Compressive stress-strain curve. (b) *In-situ* neutron diffraction patterns for the points 1-8.

Furthermore, an attempt was made to visualize the microstructural feature induced by the mechanical training. Fig. 5(a) shows a local EBSD micrograph for another trained sample, where the twinning stress in the SD was reduced to ~1.2 MPa and the final compressive loading applied perpendicular to the SD was stopped at the strain of 3%. Apparently, the initial self-accommodated broad martensite plates with various variants have disappeared and the martensite forms a simple microstructure with two distinct variants. Moreover, the easy magnetization axis of one variant is approximately parallel to the SD, and that of the other variant perpendicular to the SD, as revealed by the {0 1 0}$_{5M}$ pole figure (Fig. 5(b)). Fig. 5(c) shows the misorientation angle distribution along the black solid line drawn in Fig. 5(a). The two neighboring variants have the misorientation angle of ~94°, indicating that they are in type-II twin relation [12]. It was reported that for the single crystal Ni-Mn-Ga alloy, the twinning stress of 5M martensite with type-II twin can be as low as ~0.1 MPa [36], whereas that of type-I twin is over 1.2 MPa. Therefore, the relatively low twinning stress observed in the present directionally solidified alloy can be a direct consequence of the extensive formation of type-II twin through mechanical training.

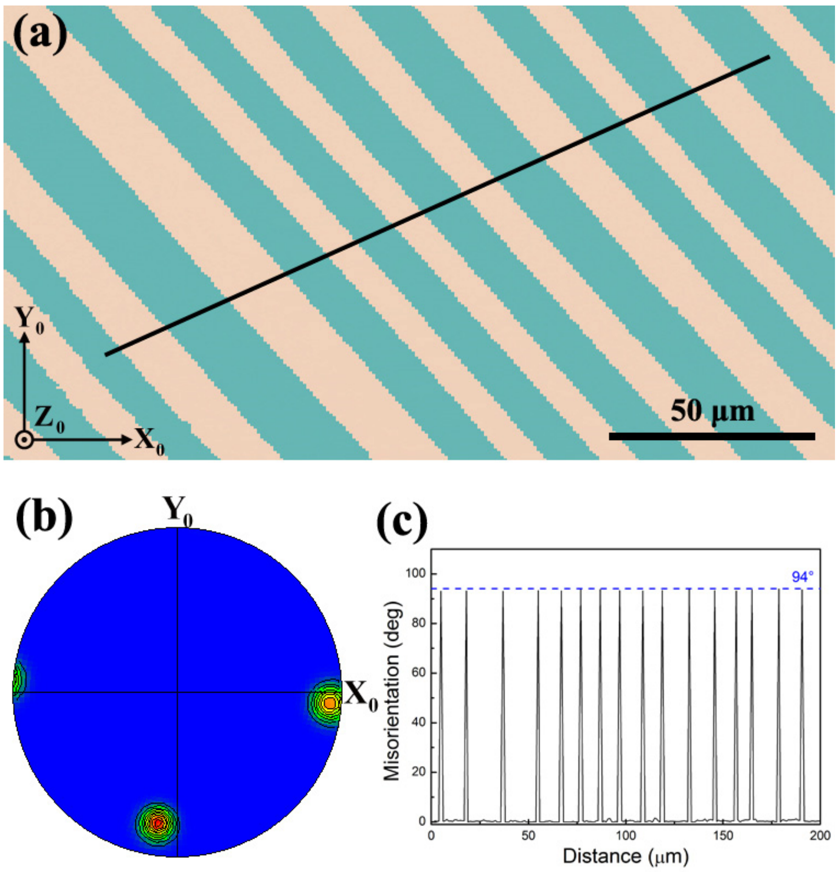

Fig. 5. (a) Local EBSD orientation micrograph of 5M martensite after mechanical training. (b) {0 1 0}$_{5M}$ pole figure determined according to EBSD measurements. (c) Misorientation profile between the neighboring variants.

3.3. Magnetic-field-induced strain

Fig. 6(a) shows the MFIS curve measured along the SD at the room temperature for an initial as-solidified sample without mechanical training, where the external magnetic field was applied perpendicular to the SD. In this case, the 5M martensite variants with $<0\ 1\ 0>_{5M}$ perpendicular to the SD should become favored, resulting in elongation in the SD. It is shown that the maximum MFIS value of 0.31% can be achieved, being higher than that in the directionally solidified $Ni_{50.5}Mn_{24}Ga_{25.5}$ alloy (*i.e.*, 0.115%) [18]. However, since the twinning stress for the initial sample without mechanical training was relatively high, the MFIS was still at a low level.

As demonstrated in Fig. 3, the twinning stress in the trained sample can be reduced to ~0.9 MPa after mechanical training, which is obviously lower than the maximum magneostress of ~2.6 MPa for 5M marteniste [20]. In this condition, large MFIS can be expected. Fig. 6(b) displays the MFIS curve measured along the SD at the room temperature for this trained sample. Because the final cycle compression was applied along the SD, the $<0\ 1\ 0>_{5M}$ easy magnetization axis was preferentially distributed along the SD. Thus, the external magnetic field was applied perpendicular to the SD in order to reorient the easy magnetization axis to be perpendicular to the SD. Notably, a maximum MFIS up to ~2.1% was obtained under a moderate magnetic field of 1 T (Fig. 6(b)). In this case, the compressive stress-favored variants (*i.e.*, $<0\ 1\ 0>_{5M}$ // SD) transform to the magnetic field-favored variants (*i.e.*, $<0\ 1\ 0>_{5M} \perp$ SD) through variant reorientation. Compared to the initial state without mechanical training (Fig. 6(a)), the MFIS level was greatly enhanced after the cyclic compressions. Such a large MFIS should arise from the coarse-grained columnar microstructure with a strong $<0\ 1\ 0>_A$ texture in the directionally solidified alloy, as well as the reduced twinning stress through mechanical training. The present MFIS value (~2.1%) is about two times higher than that reported by Gaitzsch *et al.* (*i.e.*, ~1%) in a directionally solidified $Ni_{50}Mn_{29}Ga_{21}$ alloy [20].

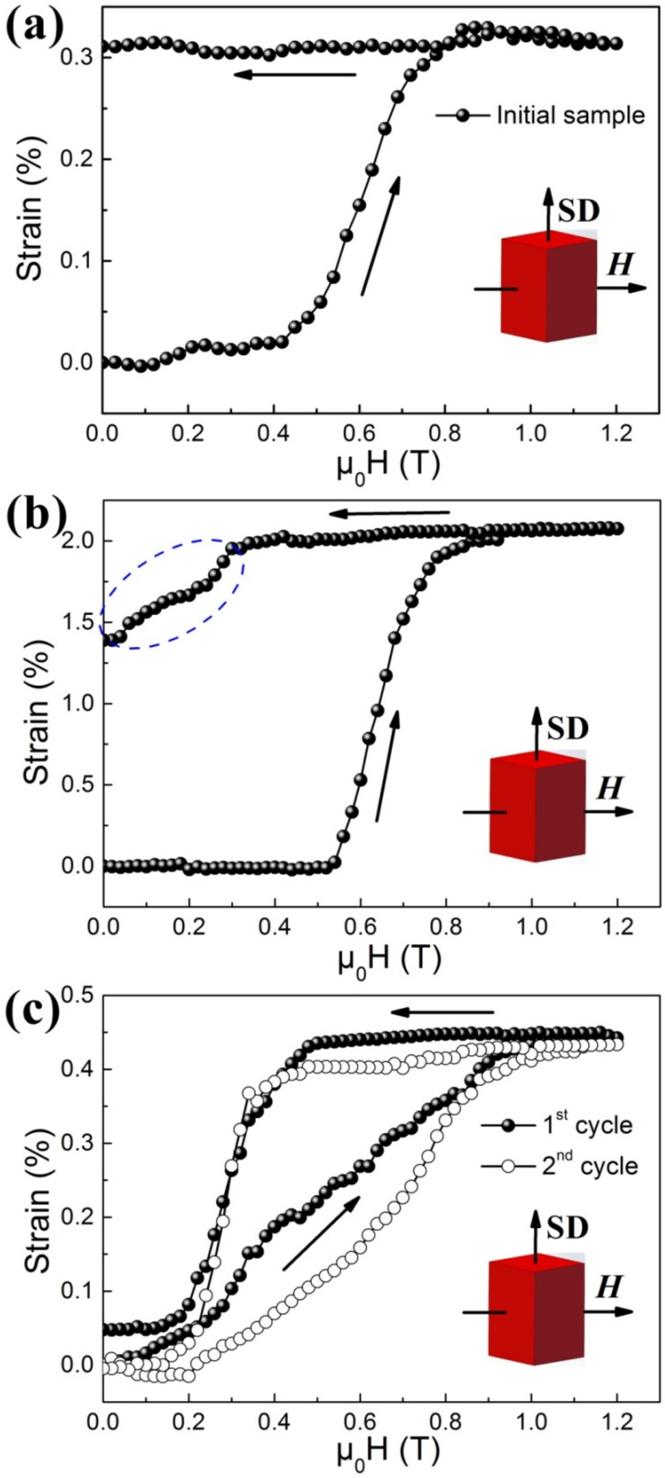

Fig. 6. (a) MFIS values as a function of magnetic field measured by laser displacement sensors along the SD for the sample without mechanical training. (b) MFIS values as a function of magnetic field measured along the SD for the sample after mechanical training. (c) Reversible MFIS values as a function of magnetic field.

As highlighted in blue dashed cycle in Fig. 6(b), certain MFIS can be recovered during the demagnetization process. In order to confirm this effect, the MFIS values were measured in additional two cycles of magnetization/demagnetization process, as shown in Fig. 6(c). In both cycles, the maximum MFIS value of ~0.4% was obtained under the magnetic field of 1.2 T. On removing the magnetic field, the MFIS was almost recovered. Thus, a reversible MFIS up to ~0.4% actuated by the magnetic field can be attained. This value is much higher than the magnetically resettable MFIS (*i.e.*, 0.16%) obtained by rotating the magnetic field by 90° in a directionally solidified $Ni_{50}Mn_{29}Ga_{21}$ alloy [19].

3.4. Origin of reversible MFIS

Generally, the field driven variant reorientation is not reversible on the removal of magnetic field for Ni-Mn-Ga single crystals. To recover the MFIS, it needs additional driving force to reorient the variants to the initial state. This could be realized through rotating the magnetic field by 90° or applying an external stress perpendicular to the magnetic field [8, 29]. In contrast, a large reversible MFIS is accessible in the present directionally solidified alloy after mechanical training, with no need of an external stress or a bias magnetic field. This distinct magnetoresponse would give polycrystalline Ni-Mn-Ga alloys more options for actuator and sensor applications.

Here, the possible origin of the observed reversible MFIS is analyzed in terms of internal stress stored in the system. As mentioned before, by the cyclic uniaxial compressions, the self-accommodated martensite is transformed to a simple configuration through reorientation or detwinning of martensite variants. During this process, certain internal stress could be introduced and stored at austenite grain boundaries [37]. Especially, as shown in Fig. 3, since the final compression was applied parallel to the SD, certain oriented internal stress along SD was considered to be introduced [38]. Such oriented internal stress may have a similar effect as that of external uniaxial stress. On the removal of the magnetic field applied perpendicular to the SD, the oriented internal stress stored in the system would drive certain amount of variants with $<0\ 1\ 0>_{5M}$ perpendicular to the SD to reorient back to the initial state with $<0\ 1\ 0>$ parallel to the SD, resulting in the reversible MFIS. Moreover, as the reversible MFIS is attainable in the mechanically trained state but not evident in the as-solidified state, the internal stress introduced by the mechanical training should be considered as the primary source.

4. Conclusions

Polycrystalline $Ni_{50}Mn_{28.5}Ga_{21.5}$ alloy with 5M martensite was fabricated by directional solidification. Results show that the original austenite formed coarse columnar-shaped grains with a strong $<0\ 0\ 1>_A$ texture. Through the repeated compressions along two perpendicular directions, the twinning stress of 5M martensite was successfully reduced to ~0.9 MPa, due to the extensive formation of type-II twin. A large one-way MFIS up to ~2.1% was achieved through the magnetic field-induced variant reorientation. Such an excellent performance should be attributed to the optimized microstructural feature and the reduced twinning stress. In addition, a reversible MFIS of ~0.4% was also obtained, where the internal stress introduced through mechanical training was considered to be the primary source for this distinct property. The present work is expected to offer some instructions for the microstructure control and property optimization of ferromagnetic shape memory alloys.

Acknowledgements

The neutron diffraction results were based upon the experiments performed at STRESS-SPEC operated by FRM II and HZG at the Heinz Maier-Leibnitz Zentrum (MLZ), Garching, Germany. The authors appreciated the MLZ Sample Environment Group for the assistance of the neutron diffraction experiments at STRESS-SPEC. This work was supported by the National Natural Science Foundation of China (Grant Nos. 51431005, 51771048, 11364035), the Fundamental Research Funds for the Central Universities of China (Grant No. N180204013), the Liaoning Revitalization Talents Program (Grant No. XLYC1907082, XLYC1802023) and the 111 Project of China (No. BP0719037).

Data availability

The raw/processed data required to reproduce these findings cannot be shared at this time as the data also forms part of an ongoing study.

References

[1] K. Ullakko, J. K. Huang, C. Kantner, R. C. O'Handley, V. V. Kokorin, Large magnetic-field-induced strains in Ni_2MnGa single crystals, Appl. Phys. Lett. 69 (1996) 1966-1968.

[2] G. H. Wu, C. H. Yu, L. Q. Meng, J. L. Chen, F. M. Yang, S. R. Qi, W. S. Zhan, Z. Wang, Y. F. Zheng, L. C. Zhao, Giant magnetic-field-induced strains in Heusler alloy NiMnGa with modified composition, Appl. Phys. Lett. 75 (1999) 2990-2992.

[3] S. J. Murray, M. Marioni, S. M. Allen, R. C. O'Handley, T. A. Lograsso, 6% magnetic-field-induced strain by twin-boundary motion in ferromagnetic Ni-Mn-Ga, Appl. Phys. Lett. 77 (2000) 886-888.

[4] A. Sozinov, A. A. Likhachev, N. Lanska, K. Ullakko, Giant magnetic field induced strain in NiMnGa seven-layered martensitic phase, Appl. Phys. Lett. 80 (2002) 1746-1748.

[5] A. Sozinov, N. Lanska, A. Soroka, W. Zou, 12% magnetic field-induced strain in Ni–Mn–Ga-based non-modulated martensite, Appl. Phys. Lett. 102 (2013) 021902.

[6] E. Pagounis, R. Chulist, M. J. Szczerba, M. Laufenberg, Over 7% magnetic field-induced strain in a Ni-Mn-Ga five-layered martensite, Appl. Phys. Lett. 105 (2014) 052405.

[7] E. Pagounis, M. J. Szczerba, R. Chulist, M. Laufenberg, Giant magnetic field-induced work output in a NiMnGa seven-layered modulated martensite, Appl. Phys. Lett. 107 (2015) 152407.

[8] P. Müllner, V. A. Chernenko, G. Kostorz, Large cyclic magnetic-field-induced deformation in orthorhombic (14M) Ni-Mn-Ga martensite, J. Appl. Phys. 95 (2004) 1531-1536.

[9] D. C. Dunand, P. Müllner, Size effects on magnetic actuation in Ni-Mn-Ga shape-memory alloys, Adv. Mater. 23 (2011) 216-232.

[10] Z. B. Li, D. Li, J. X. Chen, B. Yang, N. F. Zou, Y. D. Zhang, C. Esling, X. Zhao, L. Zuo, Crossing twin of Ni-Mn-Ga 7M martensite induced by thermo-mechanical treatment, Acta Mater. 185 (2020) 28–37.

[11] J. Pons, V. A. Chernenko, R. Santamarta, E. Cesari, Crystal structure of martensitic phases in Ni-Mn-Ga shape memory alloys, Acta Mater. 48 (2000) 3027-3038.

[12] Z. B. Li, Y. D. Zhang, C. Esling, X. Zhao, L. Zuo, Twin relationships of 5M modulated martensite in Ni-Mn-Ga alloy, Acta Mater. 59 (2011) 3390-3397.

[13] Z. B. Li, Y. D. Zhang, C. Esling, X. Zhao, L. Zuo, Composition-dependent ground state of martensite in Ni-Mn-Ga alloys, Acta Mater. 61 (2013) 3858-3865.

[14] Z. B. Li, B. Yang, Y. D. Zhang, C. Esling, N. F. Zou, X. Zhao, L. Zuo, Crystallographic insights into the intermartensitic transformation in Ni-Mn-Ga alloys, Acta Mater. 74 (2014) 9-17.

[15] S. Guo, Y. Zhang, J. Li, B. Quan, Y. Qi, X. Wang, Martensitic transformation and magnetic-field-induced strain in magnetic shape memory alloy NiMnGa melt-spun ribbon, J. Mater. Sci. Technol. 21 (2005) 211-214.

[16] N. V. Rama Rao, R. Gopalan, M. Manivel Raja, J. Arout Chelvane, B. Majumdar, V. Chandrasekaran, Magneto-structural transformation studies in melt-spun Ni-Mn-Ga ribbons, Scr. Mater. 56 (2007) 405-408.

[17] M. Pasquale, C. Sasso, S. Besseghini, F. Passaretti, E. Villa, A. Sciacca, NiMnGa polycrystalline magnetically activated shape memory alloys, IEEE Trans. Magn. 36 (2000) 3263-3265.

[18] T. Liang, C. B. Jiang, H. B. Xu, Z. H. Liu, M. Zhang, Y. T. Cui, G. H. Wu, Phase transition strain and large magnetic field induced strain in $Ni_{50.5}Mn_{24}Ga_{25.5}$ unidirectionally solidified alloy, J. Magn. Magn. Mater. 268 (2004) 29-32.

[19] M. Pötschke, S. Weiss, U. Gaitzsch, D. Y. Cong, C. Hürrich, S. Roth, L. Schultz, Magnetically resettable 0.16% free strain in polycrystalline Ni-Mn-Ga plates, Scr. Mater. 63 (2010) 383-386.

[20] U. Gaitzsch, M. Pötschke, S. Roth, B. Rellinghaus, L. Schultz, A 1% magnetostrain in polycrystalline 5M Ni-Mn-Ga, Acta Mater. 57 (2009) 365-370.

[21] L. Straka, O. Heczko, H. Hänninen, Activation of magnetic shape memory effect in Ni-Mn-Ga alloys by mechanical and magnetic treatment, Acta Mater. 56 (2008) 5492-5499.

[22] R. D. James, R. Tickle, M. Wuttig, Large field-induced strains in ferromagnetic shape memory materials, Mater. Sci. Eng. A. 273-275 (1999) 320-325.

[23] O. Heczko, Magnetic shape memory effect and magnetization reversal, J. Magn. Magn. Mater. 290-291 (2005) 787-794.

[24] U. Gaitzsch, M. Pötschke, S. Roth, B. Rellinghaus, L. Schultz, Mechanical training of polycrystalline 7M $Ni_{50}Mn_{30}Ga_{20}$ magnetic shape memory alloy, Scr. Mater. 57 (2007) 493-495.

[25] R. Chulist, W. Skrotzki, C. G. Oertel, A. Böhm, M. Pötschke, Change in microstructure during training of a $Ni_{50}Mn_{29}Ga_{21}$ bicrystal, Scr. Mater. 63 (2010) 548-551.

[26] Z. B. Li, Y.D. Zhang, C. Esling, W. M. Gan, N. F. Zou, X. Zhao, L. Zuo, In-situ neutron diffraction study of martensitic variant redistribution in polycrystalline Ni-Mn-Ga alloy under cyclic thermo-mechanical treatment, Appl. Phys. Lett. 105 (2014) 021907.

[27] H. G. Brokmeier, W. M. Gan, C. Randau, M. Voeller, J. Rebelo-Kornmeier, M. Hofmann, Texture analysis at neutron diffractometer STRESS-SPEC, Nucl. Instr. & Meth. Phys. Res. A. 642 (2011) 87-92.

[28] C. Randau, U. Garbe, H.G. Brokmeier, Stress Texture Calculator: a software tool to extract texture, strain and microstructure information from area-detector measurements, J. Appl. Cryst. 44 (2011) 641-646.

[29] H. E. Karaca, I. Karaman, B. Basaran, Y.I. Chumlyakov, H.J. Maier, Magnetic field and stress induced martensite reorientation in NiMnGa ferromagnetic shape memory alloy single crystals, Acta Mater. 54 (2006) 233-245.

[30] O. Heczko, A. Sozinov, K. Ullakko, Giant field-induced reversible strain in magnetic shape memory NiMnGa alloy, IEEE Trans. Magn. 36 (2000) 3266-3268.

[31] Z. Li, K. Xu, H. M. Yang, Y. L. Zhang, C. Jing, Magnetostrain and magnetocaloric effect by field-induced reverse martensitic transformation for Pd-doped $Ni_{45}Co_5Mn_{37}In_{13}$ Heusler alloy, J. Appl. Phys. 117 (2015) 223904.

[32] A. Saren, D. Musiienko, A.R. Smith, K. Ullakko, Pulsed magnetic field-induced single twin boundary motion in Ni-Mn-Ga 5M martensite: A laser vibrometry characterization, Scr. Mater. 113 (2016) 154-157.

[33] Z. B. Li, N. F. Zou, B. Yang, W. M. Gan, L. Hou, X. Li, Y. D. Zhang, C. Esling, M. Hofmann, X. Zhao, L. Zuo, Effect of compressive load on the martensitic transformation from austenite to 5M martensite in a polycrystalline Ni-Mn-Ga alloy studied by *in-situ* neutron diffraction, J. Alloy. Compd. 666 (2016) 1-9.

[34] Z. B. Li, Y. D. Zhang, C. Esling, X. Zhao, L. Zuo, Determination of the orientation relationship between austenite and 5M modulated martensite in Ni-Mn-Ga alloys, J. Appl. Cryst. 44 (2011) 1222-1226.

[35] Z. B. Li, B. Yang, N. F. Zou, Y. D. Zhang, C. Esling, W.M. Gan, X. Zhao, L. Zuo, Crystallographic characterization on polycrystalline Ni-Mn-Ga alloys with strong preferred orientation, Materials 10 (2017) 463.

[36] A. Sozinov, N. Lanska, A. Soroka, L. Straka, Highly mobile type II twin boundary in Ni-Mn-Ga five-layered martensite, Appl. Phys. Lett. 99 (2011) 124103.

[37] Y. D. Wang, Y. Ren, H. Q. Li, H. Choo, M. L. Benson, D. W. Brown, P. K. Liaw, L. Zuo, G. Wang, D. E. Brown, E. E. Alp, Tracing memory in polycrystalline ferromagnetic shape-memory alloys, Adv. Mater. 18 (2006) 2392-2396.

[38] E. Y. Panchenko, E. E. Timofeeva, N. G. Larchenkova, Y. I. Chumlyakov, A. I. Tagiltsev, H. J. Maier, G. Gerstein, Two-way shape memory effect under multi-cycles in [001]-oriented $Ni_{49}Fe_{18}Ga_{27}Co_{6}$ single crystal, Mater. Sci. Eng. A. 706 (2017) 95-103.